Oct 14th, 12:00 AM

Response of Metal Roofs to Uniform Static and True Hurricane Wind Loads

Ralph R. Sinno

Nineteenth International Specialty Conference on Cold-Formed Steel Structures
St. Louis, Missouri, U.S.A, October 14 & 15 2008

Response of Metal Roofs to Uniform Static and True Hurricane Wind Loads

By
R. Ralph Sinno, Ph.D., P.E., F. ASCE*

Abstract

The primary objective of this work is two fold: (1) Development of a test method that simulates the non-uniform unsteady wind loading conditions in time and space on a roof of a low rise building. This is done using electromagnetic controlled uplift pressures, suction, on metal roofs. (2) To establish a comparative correlation between the current uniform static loading used for design and the true hurricane dynamic uplift wind loading. This is the first time ever that the wind tunnel data for the footprint of true hurricane wind loading is duplicated and applied successfully to full-scale roofs in the laboratory. The test results confirmed that the maximum anchoring reactions are almost proportional to the square of the wind speed under static and simulated true wind loading. These reactions are considerably lower under true wind loading than those from the ASCE-7-05 for uniform static loading. Deflections and deformations of end panels of the roof are noted to be excessively higher under true wind loading than those under uniform static loading. Test results and findings are applicable to any type of roof system and materials used to construct and build roofs in real life.

1.0 GENERAL

The primary objective of this research is the simulation of wind tunnel loading data applied to standing seam thin sheet metal roofing. Evaluation and prediction of the clip reactions of full scale metal roofs subjected to uniform static loading and simulated wind tunnel loading is presented. Vertical legs and

*Professor of Civil Engineering, P.O. Box 9546, MSU, MS 39762, Telephone 662-325-3737, E-mail sinno@engr.msstate.edu

trapezoidal standing seam roofs were used. The test results from simulated wind loading are compared to those results from uniform static loading. Uniform static loading followed the ASTM E-1592-01[2] testing procedures. The work reported here covers, in general, metal roofing commonly used by the metal building industry in the U.S.

Laboratory testing using uniform static loading conditions induced by compressed air or partial vacuum are presently used to verify the structural performance of thin metal standing seam roofs. This air pressure difference loading method for testing does not represent, or even come close to simulate, the true wind loading spectrum in the time and space. Under uniform static loading, the metal roofs usually swell to a balloon shape with severe uniform unlocking pressure on the standing seamlines of the panels. Accordingly, the test results from using uniform static loading have been the center of continuous appraisals by structural engineers, wind engineering specialists, hazards mitigation experts, forensic investigators, and scientific researchers. Field surveys of wind loading on roofs in real life have confirmed the seriousness of this disparity.

2.0 BACKGROUND

The most sophisticated testing device available for testing metal roofs, other than the uniform static loading, has been the BRERWULF test setup. This test was developed by Cook, Keevil, and Stobart [4]. The unsteady pressures produced in this test set-up remain spatially uniform.

Clemson University used the BRERWULF to re-create dynamic hurricane level winds in the laboratory [5]. The tests were successful in evaluating boundary effects and the variability of clip influence surfaces. However, the peak effective pressures were too small to provide insight into clip loading and roof behavior before failure.

3.0 THE CURRENT APPROACH FOR DESIGN OF METAL ROOFS

The current standard design procedure for design of metal roofs for wind loading is based on statistical averages of wind tunnel data using weighted factors related to the location and terrain. To reduce the complexity of the pressure variations, the current ASCE-7 design procedure specifies that metal buildings should be designed for uniform pressures over pressure zones: interior, edge, and corner zones.

The calculated static uniform clip reactions in comparison to those caused by true wind loading remain questionable. In spite of the seriousness associated with the magnitude and steadiness of these reactions, they are used for the design of the framing and foundations that support the entire metal building.

4.0 OBJECTIVE OF THE RESEARCH

The primary objective of this research work has been two fold:

1) Develop a test method that simulates the non-uniform unsteady wind loading conditions in time and space on a standing seam metal roofing. Suction on metal roofing using electromagnetic controlled uplift pressures was developed in a previous MBMA research project (6). The details for loading using induce electromagnetic uplift pressures including its velocity can be found in Reference (7).

2) Establishing a correlation between the current uniform static testing and the dynamic electromagnetic uplift testing. This comparative study addressed also the comparative performances of the roofs under load up to failure.

5.0 TESTING PROGRAM

The testing program was basically two parts:

1) Test typical roofs using uniform static pressure difference as per ASTM 1592-01 protocol.

2) Test the same roof layout under electromagnetic uplift loading up to failure.

The testing program was executed on two roof profiles; vertical legs and trapezoidal. The tested vertical legs profile was 16 in. panel, 24 guage metal roofing, span 5’ 1”, and it was provided by a Houston, Texas, metal building manufacturer. Four vertical legs roofs were tested under uniform static pressure and two identical roofs were tested under electromagnetic uplift UWO wind tunnel simulation loading. The roofs were supplied and installed by corresponding metal building manufacturer duplicating all details procedures used by each in a real full scale filed installation.

Two roofs made of 24 ins. wide trapezoidal panels were also tested. One roof was provided by a Houston, Texas metal building manufacturer with a metal thickness of 24 guage, while the other roof was provided by CECO Building Systems using 22 guage for the metal thickness. Both trapezoidal roofs were installed on 5'-1" purlin spacing. Only the test results on the vertical legs profile are reported here, and for additional coverage and test results on these tests, see References 9 and 10.

6.0 TEST SET-UPS

6.1 Static Tests-ASTM E-1592

The uniform static loading test set-up followed the ASTM E 1592-02 loading sequences and procedure.

Tests were also performed independently by each metal building manufacturer that supplied these roofs at their own facilities, and the findings were compared and found to confirm each other.

The main interest of running the static tests was to create a reference file on the performance of the roofs under uniform static loading that could later be used for comparison with electromagnetic uplift testing. The load deflection curves for loading and unloading and the load transfer reactions at the clips were of primary interest.

All tested roofs were made of galvalume sheet metal roofing commonly used by the metal building industry in the U.S. All roofs were made of five panels, 20'- 4" long, supported on 5 purlins spaced at 5'- 1".

6.2 Electromagnetic Uplift Test Set-Up

Non-uniform dynamic uplift forces were produced by using intense electromagnetic suction force from suspended magnets at a gap distance from the metal roof. Extensive research on the efficiency and optimization of the induced electromagnetic uplift forces in the grid system was required to develop the electromagnets used in this study [6].

Magnetic nodal points were placed on top of the roof at variable gap distances and suspended form 8 overload beams. The layout of the 34 electromagnetic nodal points was established on the basis of the data provided by the UWO Wind Tunnel Tests.

The induced electromagnetic uplift forces were then programmed to simulate a given wind tunnel data file. University of Western Ontario boundary layer wind tunnel data were used to generate the simulated non-uniform dynamic wind loading for each electromagnet. These uplift suction forces were applied by each electromagnetic actuator at the centroid of the area as designated by the UWO wind tunnel data. Each nodal point consisted of the actuator, an electronic control board, and a load cell for verification of the force produced. The system was programmed to generate time varying forces equivalent to the forces supplied by UWO. See Figures. 1 to 5 for the electromagnetic test setup and details of related parts.

Fig 1. Electromagnetic Nodal Point - Magnet.

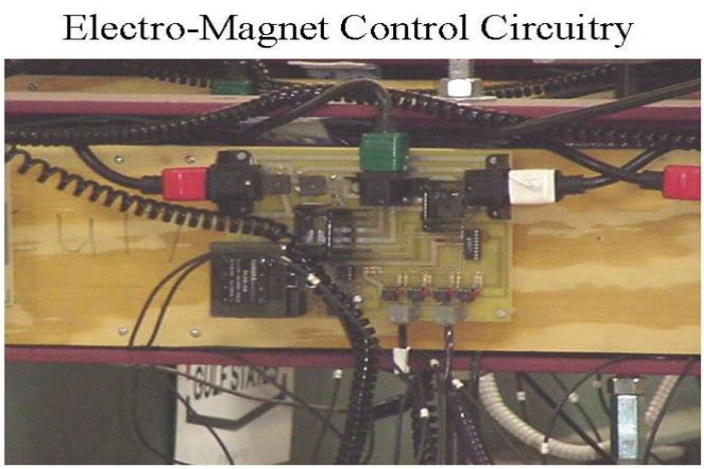

Fig 2. Electromagnetic Nodal Point - Control Panel Board Circuitry

Fig 3. Electromagnetic uplift Testing - Group of Electromagnetic Nodal Points

Fig 4. Electromagnetic uplift Testing - Front View of 34 Nodal Points Placed as per UWO Area Distribution

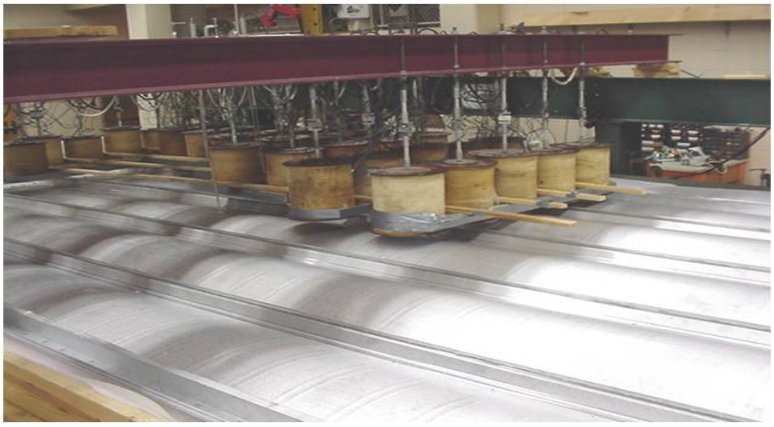

Fig 5. Electromagnetic uplift Testing - Back View

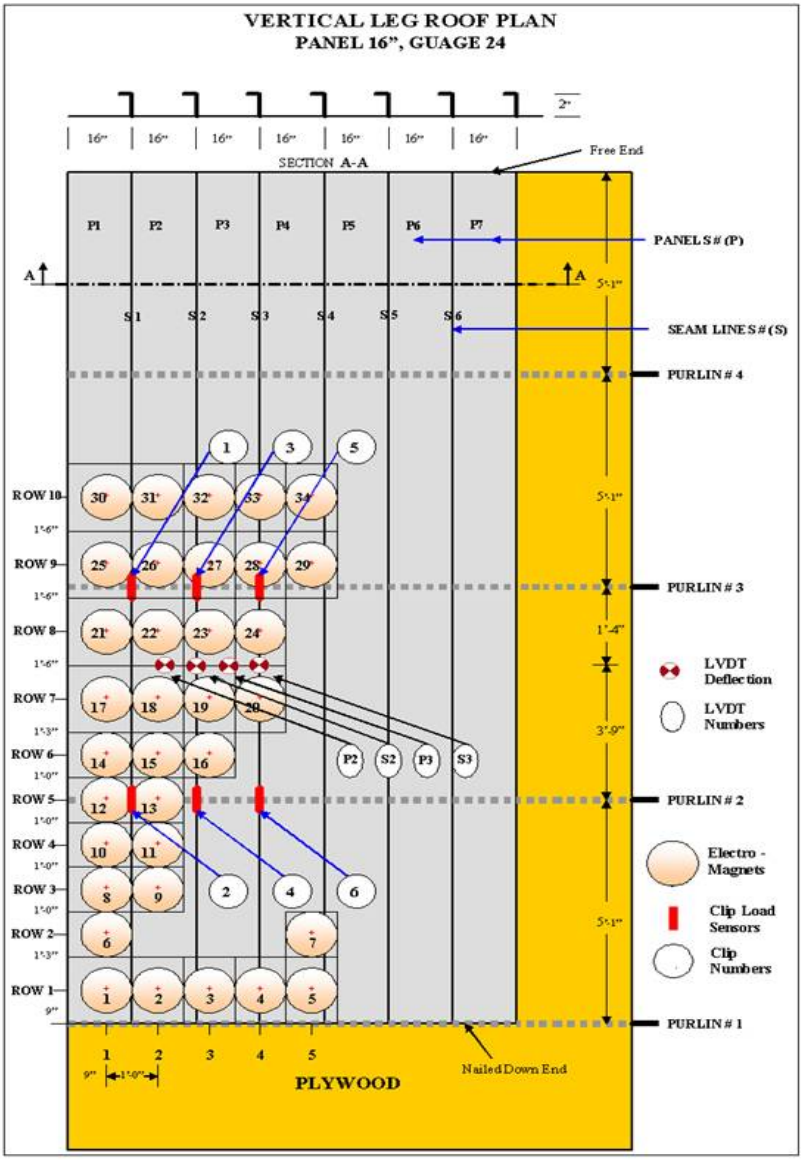

Fig 6. Electromagnetic Uplift Testing. Labeling, Instrumentation and Test Setup for Houston Vertical Legs Roofs

7.0 INSTRUMENTATION

The experimental setups of the roof layouts used for the static and electromagnetic uplift tests are shown in Figure 6 for the vertical legs roofs. This setup meets the requirements for a standard full scale testing as specified by the ASTM E-1592. This setup was used to acquire data for both the static and electromagnetic uplift tests so that a direct correlation could be drawn between the two sets of data. The Figure shows the labeling of all panels and seam lines, location of each of the thirty four magnets, location of LVDT's for deflection measurements and labeling of the six load cells attached to the clips for recording the reactions.

7.1 Static Test ASTM E-1592

Electronic data acquisition was used exclusively in this test setup. All sensors were read at 20Hz (20 readings per second) during the entire period of testing. The following electronic sensors were used:

- A pressure transducer for monitoring the uplift air pressure inside the pressure chamber. The collected data in each test was constantly checked against a pressure differential piezometer to confirm the accuracy of the electronically recorded readings.

- Linear Variable Differential Transducers (LVDT).
  Four LVDT were used for deflection measurements placed at the center of two panels and at the tip of two adjacent seam lines.

7.2 Electromagnetic Uplift test

The following is the description of the electronic instrumentation that was also read at 20Hz (20 readings per second) during the entire period of testing under electromagnetic uplift loading:

- A pressure transducer for monitoring the uplift air pressure inside the pressure chamber. The collected data in each test was checked against a pressure differential piezometer to confirm the accuracy of the readings.

- Load cells at each electromagnetic nodal point.
  The induced uplift suction forces created by the electromagnetic field were recorded using load cells that were secured to each magnetic

nodal point. These load cells were protected from the influence of surrounding magnetic field.

- Load cells for monitoring the clip reactions.
  A total of six load cells placed on six clips on two purlins were used. The clips on Purlin Two carried even numbers (clip #2, #4, and #6), and odd numbers (clip #1, #3, and #5) were given to the clips on Purlin Three.

- LVDT (Linear Variable Differential Transducers).
  Four LVDT were used for deflection measurements placed at the center of two panels and at the tip of two adjacent seam lines.

8.0 UWO TEST DATA

The UWO data were developed using the most critical angle for loading with 110 miles per hour fastest-mile wind velocity at thirty three feet above the ground. The data were provided at 20 Hz for each area corresponding to the thirty four magnetic nodal points. The UWO area numbering, identification of wind load distribution and statistical highlights of the wind data used are shown in Figures 7 and 8, respectively.

UWO WIND DATA FOR 110MPH

(1)	(2)	(3)	(4)	(5)	(6)	(7)	(8)	(9)
Area Number	Identification	Negative Peak Load (lbs)	99 percentile Load (lbs)	Positive Peak Load (lbs)	Mean Load (lbs)	% of time signals are suction	Backing Force (due to backing pressure over the area)	% of time signals exceeded 250 lbs
1	101 (1.5'x1.5')	-274.3	-136.9	43.7	-44.8	93.9	51.5	0.02
2	104 (1'x1.5')	-124.2	-73.1	31.8	-12	69.6	34.3	0
3	106 (1'x1.5')	-123.2	-83.4	30.7	-18	75.8	34.3	0
4	108 (1'x1.5')	-125.7	-79.3	31.5	-15.9	74	34.3	0
5	110 (1'x1.5')	-129.1	-82	30.6	-16.5	74.7	34.3	0
6	401 (1.5'x1')	-233.8	-139.2	31.4	-46.8	96	34.3	0
7	410 (1'x1')	-49.4	-25.9	24.7	6.2	19.2	22.9	0
8	601 (1.5'x1')	-239.7	-146.6	26.8	-55.7	98.5	34.3	0
9	604 (1'x1')	-69.7	-30	26.2	6	17.3	22.9	0
10	801 (1.5'x1')	-259.1	-150.7	24.6	-57.3	98.6	34.3	0.02
11	804 (1'x1')	-105.4	-51.6	24.6	-5.2	56.3	22.9	0
12	1001 (1.5'x1')	-236.8	-151.8	24.2	-59.4	99	34.3	0
13	1004 (1'x1')	-132.9	-66.5	24.1	-16.5	84	22.9	0
14	1201 (1.5'x1')	-209.9	-137.5	22.6	-54.2	99.2	34.3	0
15	1204 (1'x1')	-142.3	-74.7	22	-22.3	92.5	22.9	0
16	1206 (1'x1')	-79.9	-40.4	26.9	4.9	25.2	22.9	0
17	1401 (1.5'x1.5')	-264.9	-182.7	36.1	-70	99	51.5	0.05
18	1404 (1'x1.5')	-206.1	-122.8	29.1	-40.2	95.7	34.3	0
19	1406 (1'x1.5')	-165.7	-78.5	40.4	-6.1	51.1	34.3	0
20	1408 (1'x1.5')	-119	-61	50.4	13.6	17.9	34.3	0
21	1701 (1.5'x1.5')	-216.3	-156.6	33.6	-57.7	98.5	51.5	0
22	1704 (1'x1.5')	-180.2	-124.6	27.5	-44.8	97.9	34.3	0
23	1706 (1'x1.5')	-188.6	-98.6	37.6	-23.5	80.3	34.3	0
24	1708 (1'x1.5')	-185.2	-85.9	46.1	-3.2	44.9	34.3	0
25	2001 (1.5'x1.5')	-201.4	-137.2	36.7	-48.7	97.5	51.5	0
26	2004 (1'x1.5')	-169.5	-112.4	27.6	-41.5	98.4	34.3	0
27	2006 (1'x1.5')	-166.5	-107.3	34.6	-32.1	91.1	34.3	0
28	2008 (1'x1.5')	-187.7	-101.9	41.7	-19	68.1	34.3	0
29	2010 (1'x1.5')	-121.5	-62.8	40.3	-5.8	57.4	34.3	0
30	2301 (1.5'x1.5')	-183.7	-118.1	38.9	-37.9	94	51.5	0
31	2304 (1'x1.5')	-174.6	-103.3	29.4	-36	97.7	34.3	0
32	2306 (1'x1.5')	-191.4	-110.2	32.2	-35.5	94.7	34.3	0
33	2308 (1'x1.5')	-182.3	-110.7	43.4	-29.8	82.8	34.3	0
34	2310 (1'x1.5')	-177.9	-105.5	42.1	-27.4	81.3	34.3	0
35	2601 (1.5'x1.5')	-157.6	-101.6	38.2	-31	90.9	51.5	0
36	2604 (1'x1.5')	-135.9	-84.5	28.2	-27.6	95.8	34.3	0
37	2606 (1'x1.5')	-149.3	-93.2	30.2	-30.6	96.6	34.3	0
38	2608 (1'x1.5')	-133.5	-80.3	33.1	-19.6	82.1	34.3	0
39	2610 (1'x1.5')	-122.2	-62.7	40.5	-0.4	45.3	34.3	0

All values are based on an applied backing pressure of 22.9 psf.

Fig 7. Statistics of Wind Load Data for the 39 Nodal Points at 10 mph – Provided by UWO

UWO WIND LOAD DISTRIBUTION AT 110MPH

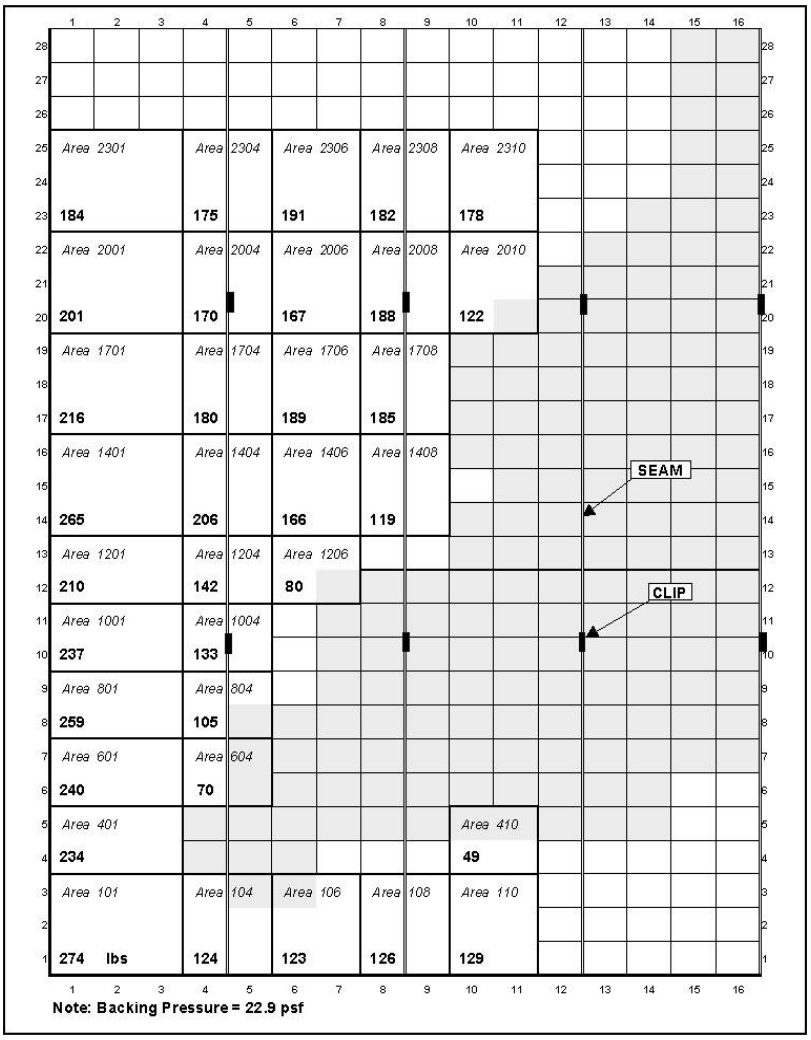

Fig 8. Wind Load Distribution at 110 mph – Mapping from UWO Wind Tunnel Data

9.0 UNIFORM STATIC PRESSURE TESTS – ASTM E-1592

Four full-scale vertical legs roofs were tested. The roof panel profile and layout were selected to withstand a design uplift wind load of 30-35 psf. The roofs were 16'' panels, 24 guage galvalume grade 50 ksi steel metal sheets, and placed at 5'-1'' purlin spacing. The tests were carried up to the ultimate failure load of the roof. See Figures 9, 10 and 11 for selected views of the tested vertical legs roofs.

These tests provided a reference file on the performance of the roof under uniform static loading. This will be used for comparison and correlation with the dynamic simulated electromagnetic uplift wind loading. The load deflection curves for loading and unloading and the clip anchorage reactions were recorded in these tests.

Clip reactions for all 4 roofs are shown on Figures 12 and 13, respectively.

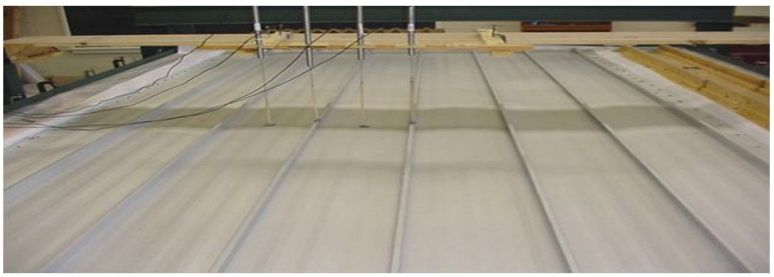

Fig 9. Uniform Static Pressure Tests- ASTM E-1592. Houston Vertical Legs Roofs – Before Loading.

Fig 10. Uniform Static Pressure Tests- ASTM E-1592. Houston Vertical Legs Roofs – During Loading.

Fig 11. Uniform Static Pressure Tests- ASTM E-1592. Houston Vertical Legs Roofs – After Failure of Seamline.

The clip reactions for the six instrumented clips are shown with the Tributary Area Line to show that the experimental collected and recorded clip reactions are within the rough estimate of the tributary area design approach. The deviation of the measured data from the tributary line can be attributed to the boundary conditions of the panels and to the roof deformation as a whole. It is interesting to note that the roof responded linearly to the uniform static pressure loading as verified by the linearity of the recorded clip reactions up and until failure. Recorded clip reactions indicated that load redistributed between clip reactions did occur at the instance of seam or clip failure.

It should be noted that roofs #1 and #2 were installed in an awkward manner by using partial pieces of a full panel for the first and last panels in the roof layout. This awkward installation was corrected in roofs #3 and #4 by using the full 16'' width of the panel on all five panels of the roof. Roofs #3 and #4 will be used for comparison with electromagnetic uplift testing because they were installed identically to each others in both tests.

Figures 9 and 10 show the average clip loadings for roofs #1 and #2, and roofs #3 and #4, respectively, with the Tributary Area Lines. The average of roofs #3 and #4 compare extremely well with the expected data as shown by the plot of the Tributary Area Lines. All the roofs failed at almost exactly the expected design loads. The average of the static uniform failure pressure for these two roofs is 32 psf. It is interesting to note that clip reactions on purlin #2, (clips 2, 4 and 6), are higher than clip reactions on purlin #3, (clips 1, 3 and 5). This is to be expected because it agrees with the structural analysis.

The failure mode for all roofs under uniform static load was the same for all tests. The ultimate failure of the roof corresponded to seam line failure and loss of its integrity under load.

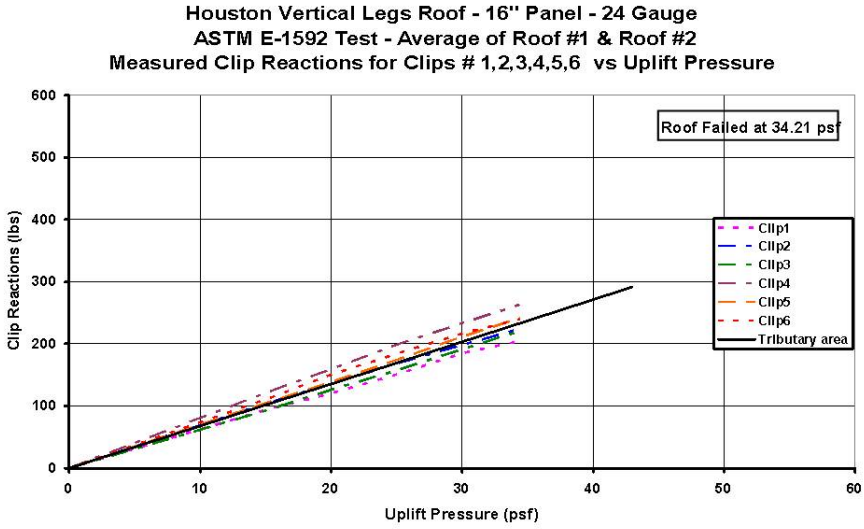

Fig 12. Uniform Static Pressure Tests-ASTM-1592. Clip Reactions - Average of Roof #1 & Roof #2

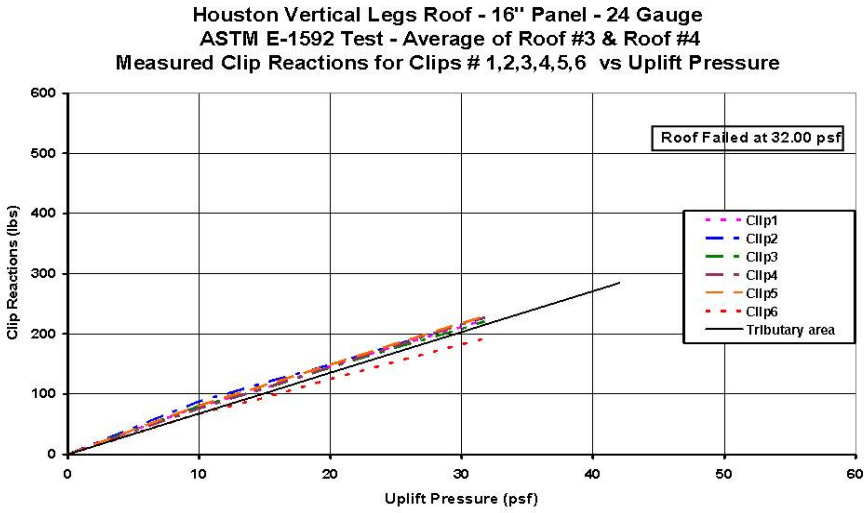

Fig 13. Uniform Static Pressure Tests-ASTM-1592. Clip Reactions - Average of Roof #3 & Roof #4

10.0 ELECTROMAGNECTIC UPLIFT TESTS

The UWO wind tunnels loading data and the applied electromagnetic forces, after completing calibration, are shown for selected nodal points in Figures 14 and 15 for nodal points #21 and #30, respectively. These plots are shown here as typical examples. In general, all nodal points matched well with the UWO wind tunnel loading in time and space. The simulation exceeded all expectations. Detailed review and evaluation was prepared by Dr. Eric Ho of Davenport Wind Engineering Group, London, Ontario, Canada, for the accuracy of simulation, and he concluded that the correction between the wind tunnel loading and that of the electromagnetic held is accurate and exceptionally acceptable for all practical purposes.

The major difficulty in simulating the UWO wind tunnel data was in duplicating extremely high spikes in loading that lasted less than one second in time duration. Further research confirmed that the mismatch was related to the roofs not responding to less than one second duration of spikes loading effectively in time and to be reflected by measurements at the clip reaction.

Response to electromagnetic uplift testing was recorded at 20Hz for the six instrumented clips and the four LVDT deflection measurements.

The clip reactions for selected wind speeds and clips are shown in Figures 16 and 17. The clip reactions for roof #1 are superimposed on those from roof#2 to show the repetitiveness of the measured test data. As shown in Figures 16 and 17, the clip reactions from both roofs did indeed repeat themselves for the same wind speed over the entire loading period. For complete data for all instrumentations and comparative analysis of all measured data for the Houston vertical legs roofs under electromagnetic testing are included in Reference 9.

Vertical leg roofs under electromagnetic uplift testing failed at maximum clip reaction, clip #1, by slippage of the clip and final disengagement from the seam line. The clip slippage propagated into seam line failure from clip #1 to clip #2. See Figures 18 and 19. For multimedia presentation for the roof under loading up to failure see Reference 9. Roof #1 and roof #2 failed at the wind speed of 70 mph.

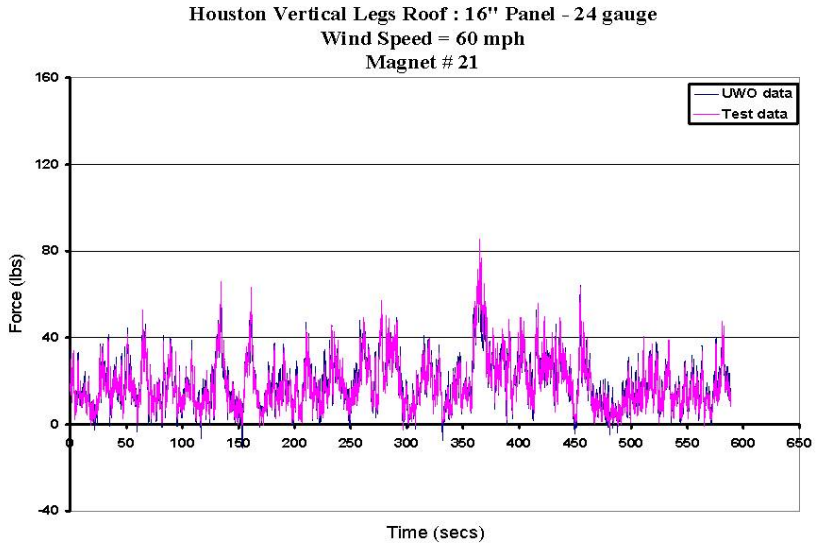

Fig 14. Electromagnetic Uplift Test Data and UWO Wind Tunnel Data Compared at 50 mph Wind - Nodal Point #21

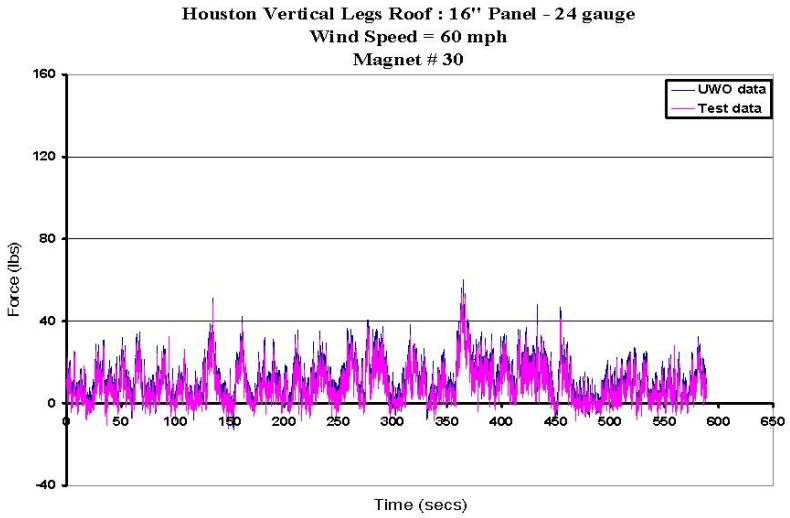

Fig 15. Electromagnetic Uplift Test Data and UWO Wind Tunnel Data Compared at 50 mph Wind - Nodal Point #30

The clip reactions for selected wind speeds for clip #1 are shown in Figures 16 and 17, roofs 1 and 2, respectively. These clip reactions for roof #1 are superimposed on those from Roof #2 to show the repetitiveness of the measured test data As shown in Figure 18 and 19 for clips #1 and #2, respectively, the clip reaction from both roofs did indeed repeat themselves for the same wind speed over the entire loading period.

Vertical leg roofs under electromagnetic uplift testing failed at maximum clip reaction, clip #1, by slippage of the clip and final disengagement from the seam line. The clip slippage propagated into seam line failure from clip #1 to clip #2. See Figures 20 and 21.

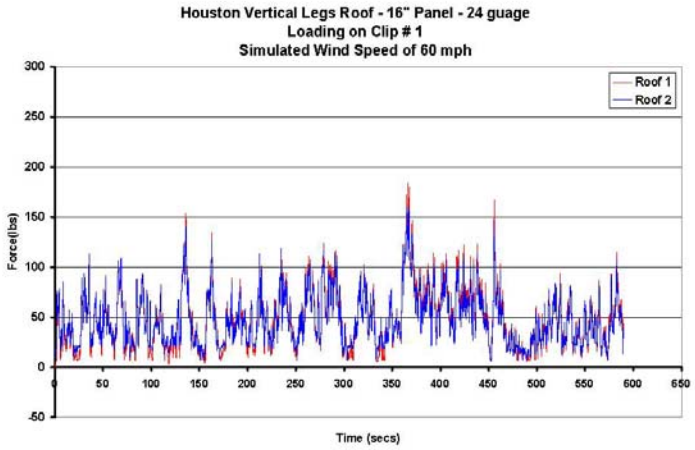

Fig 16. Comparison of Clip Reactions for Roof 1 & Roof 2 at 60 mph Wind - Clip #1

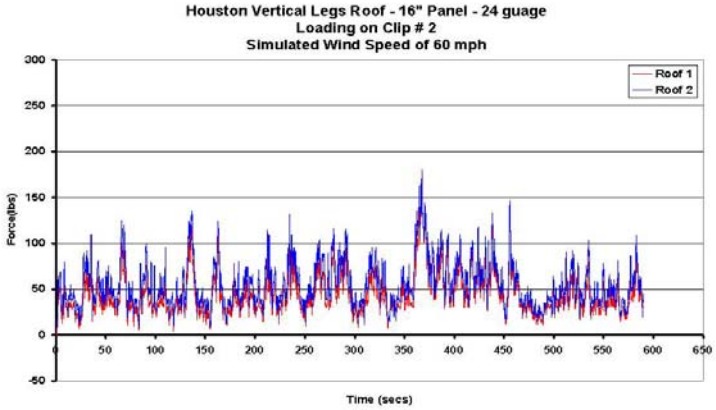

Fig 17. Comparison of Clip Reactions for Roof 1 & Roof 2 at 60 mph Wind - Clip #2

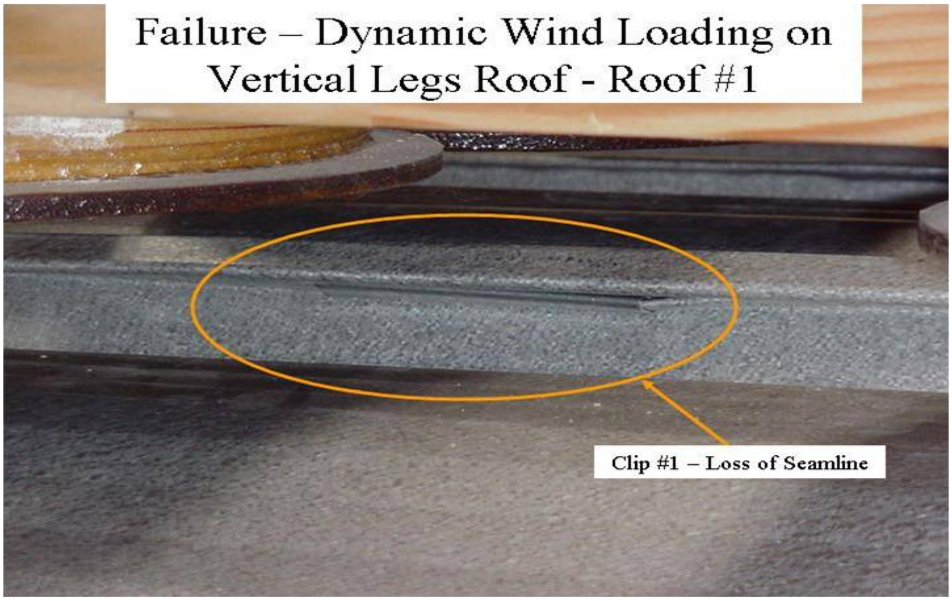

Fig 18. Failure of Clip #1 in Vertical Legs Roofs - Roof 1

Fig 19. Failure of Clip #1 in Vertical Legs Roofs - Roof 2

11.0 INDEX FACTOR

The index factor was created for design purposes in order to compare the uniform static pressure testing to electromagnetic uplift testing. This factor relates the maximum clip reaction in both tests. For the uniform static pressure test, ASTM 1592-02, the maximum clip reaction can be calculated from the maximum tributary area using ASCE 7-02 pressure loading under fastest mile wind speed with conversion to three second gust. The maximum recorded dynamic clip reaction using simulated UWO wind loading from the electromagnetic uplift test was then used in calculating the index factor. The magnitude of the clip reactions are also a reflection of the integrity of the adjacent seam lines. Thus, the index factor is defined as follows:

$$\textbf{I. F. (at any wind speed)} = \frac{\textbf{Clip Reaction using ASCE-7 and Tributary Area}}{\textbf{Maximum Recorded Dynamic Clip Reaction}} \quad \textbf{(Eq. 1)}$$

For all practical design purposes, the above calculations for the index factor, based on its definition, are approximately equal to:

$$\text{I. F.}_{(approx)} = \frac{(\text{Failure Wind Speed})^2_{\text{Dynamic}}}{(\text{Failure Wind Speed})^2_{\text{ASTM E- 1592}}} \quad \textbf{(Eq. 2)}$$

or

$$\text{I. F.}_{(approx)} = \frac{\text{Dynamic Failure Pressure}}{\text{ASCE-7 Uniform Failure Pressure}} \quad \textbf{(Eq. 3)}$$

The approximate ratios for calculating the index factor are shown only to demonstrate a simple and fast relationship between uniform static testing, ASTM 1592-02, and real world wind loading.

The calculations for the average index factor for the vertical legs roofs is shown below, and in Table 1 for intermediate loadings:

Average of roofs 1&2 (See Table 1)

$$\text{I. F.}_{(\text{average})} = \frac{\text{Clip Reaction uniform Pressure ASCE 7 X Tributary area}}{\text{Measured Maximum Dynamic Clip Reaction}} = 1.396$$

The above compare closely using the square of equivalent failure wind speeds or wind pressures:

$$\text{I. F.}_{(\text{approx})} = \frac{(\text{Failure Wind Speed})^2_{\text{Dynamic}}}{(\text{Failure Wind Speed})^2_{\text{ASTM E- 1592}}} = \frac{(70\ \text{mph})^2}{(59\ \text{mph})^2} = 1.407$$

$$\text{I. F.}_{(\text{approx})} = \frac{\text{Dynamic Failure Pressure}}{\text{ASCE-7 Uniform Failure Pressure}} = \frac{44.05\ \text{psf}}{31.31\ \text{psf}} = 1.407$$

TABLE 1: Index Factors for Roof #1 and Roof #2

Average of Roof #1 & 2

Wind Speed (mph)	Roof #1 Index Factor (Static/Dynamic)	Roof #2 Index Factor (Static/Dynamic)	Roof #1&2 Average
0	0	0	0
50	1.3254	1.3784	1.351
60	1.3124	1.481	1.396
70	1.4825	1.4197	1.451
		Average	1.396

12.0 SUMMARY AND CONCLUSIONS

The electromagnetic uplift loading test based on the gap suspension of magnetic suction forces for applying in the simulated wind tunnel loading to real full scale thin metal roofs has proven its applicability and validity in this research. The applied loading data compared favorably and exceptionally well to the pre-assigned defined wind tunnel data in time and space. The success of the simulation of wind tunnel data on full scale metal roofs, built as per standard practice of the manufacturer of these roofs, was checked also against the correlation coefficients of the wind tunnel data itself. The applied simulated electromagnetic data was found to match the UWO wind tunnel data not only in time and space but also to duplicate the correlation coefficients of the wind tunnel data. Simulated loading for wind speeds from 50mph up to 160mph were applied and monitored at the rate of 20Hz. The measured clip reactions and deflections allowed for a comparison with those recorded using statistic uniform loading, ASTM E 1592 - 02.

This was the first time ever that the wind tunnel loading data was duplicated and applied successfully to a full scale thin metal roof test setup in the laboratory. The findings from this simulation allowed detailed analysis of the anchorage clip reactions for different profiles of roofs and from different manufacturers. Duplicate tests on each type of roof were conducted and measured data confirm repetitiveness of test results.

The following conclusions can be made:

1. The test results confirmed that the maximum anchoring reactions are almost proportional to the square of the wind speed under static and simulated true wind loading.

2. The anchoring reactions are considerably lower under true wind loading than those from the ASCE-7-05 for uniform static loading.

3. Failure modes of the tested roofs under simulated wind loading differ from those under static loading as they reflect the seriousness of the high intensity of wind loading at and around the roof corners.

4. Deflections and deformations of end panels of the roof are noted to be excessively higher under true wind loading that those under uniform static loading.

5. These approaches, test results, and findings presented here are applicable to any type of roof system and materials used to construct and build the roof in real life.

ACKNOWLEDGEMENT

The research on electromagnetic uplift testing to simulate data generated by high wind velocity from wind tunnel testing has been sponsored for the past several years by the Metal Building Manufacturer's Association (MBMA), and the American Iron and Steel Institute (AISI). Also, partial funding was provided by Metal Construction Association (MCA), and FM Global.

The findings, conclusions, and opinions that are presented and expressed in this Report are those of the writer and are not necessarily those of the sponsors, MBMA, AISI, MCA, or FM.

REFERENCES

1. Ho, E., Surry, D., and Davenport, A. (1992), "Roof Uplift Testing", MBMA Research Project, Boundary Layer Wind Tunnel Laboratory. The University of Western Ontario. London, Ontario, Canada.

2. ASTM (2001). "Standard Test Method for Structural Performance of Sheet Metal Roof and Siding Systems by Uniform Static Air Pressure Difference, ASTM E-1592-01.

3. ASCE 7-05 (2005). "Minimum Design Loads for Building and Other Structures." ASCE, Reston, VA.

4. Cook, N.J., Keevil, A.P., and Stobart, R.K. (1980). "BRERWULF- The big bad wolf." J. Wind Eng. Ind. Aerodyn., 29, 99-107.

5. Prevatt, David, and Scott Schiff (1996). Uplift Testing of Standing Seam Metal Roof Systems. Clemson University. Clemson, South Carolina.

6. Sinno, R., Nail, J., and Fowler, S. (2001). "Simulation of non-uniform unsteady wind pressures." MBMA Final Report, Civil Engineering Department, Mississippi State University, MS.

7. Shaunda L. F. (2001), "Clip reactions in standing seam roofs of metal buildings", Mississippi State University, M.S. Thesis.

8. Sinno, R., Surry, D., Flower, S., and Ho, E. (2003), "Testing of Metal Roofing Systems Under Simulated Realistic Wind Loads", Proceedings Eleventh International Conference on Wind Engineering, Lubbock, Texas, pp.1065-1071.

9. Sinno, R., "Simulation of Uplift Loading on Thin Metal Roofs (Electromagnetic Uplift Testing)," MBMA Final Report, Dec. 2005.

10. Surry, David, et. al., "Structurally Effective Static Wind Loads for Roof Panels," Journal of Structural Engineering, ASCE, June 2007, pp. 871-885.